

# New Physics effects in $R(K^{(*)})$ , $B_s \rightarrow \mu^+\mu^-$ , and $B^+ \rightarrow K^+\nu\bar{\nu}$

Jong-Phil Lee\*

*Sang-Huh College, Konkuk University, Seoul 05029, Korea*

## Abstract

We analyze possible new physics (NP) effects on  $b \rightarrow s$  transition processes,  $R(K^{(*)})$ ,  $B_s \rightarrow \mu^+\mu^-$ , and  $B^+ \rightarrow K^+\nu\bar{\nu}$  decays. Though recent data for  $R(K^{(*)})$  and  $\text{Br}(B_s \rightarrow \mu^+\mu^-)$  are compatible with the standard model (SM), there are still rooms for NP beyond the SM. Especially  $\text{Br}(B^+ \rightarrow K^+\nu\bar{\nu})$  is measured to exceed the theoretical predictions. We parameterize the NP effects in a generic way with explicit NP scale  $M_{\text{NP}}$  and some possible powers of it. For reasonable ranges of NP fermionic couplings we find a window of  $3.17 \text{ TeV} \leq M_{\text{NP}} \leq 14.9 \text{ TeV}$  for new particles. Implications of our analysis about specific NP models are discussed.

arXiv:2502.06370v1 [hep-ph] 10 Feb 2025

---

\* jongphil7@gmail.com

## I. INTRODUCTION

Flavor changing neutral currents (FCNCs) are very important to the standard model (SM) of particle physics because they provide a strong and useful testbed for new physics (NP) beyond the SM. In the SM, FCNC processes are induced by loop and further suppressed by CKM factors and thus very sensitive to NP contributions.

Until recently, the ratio of the branching ratios

$$R(K^{(*)}) \equiv \frac{\text{Br}(B \rightarrow K^{(*)}\mu^+\mu^-)}{\text{Br}(B \rightarrow K^{(*)}e^+e^-)} , \quad (1)$$

showed some deviations from the SM, casting a puzzle of lepton universality violation [1–3]. But new experimental data from the LHCb [4, 5]

$$R(K)_L = 0.994^{+0.094}_{-0.087} , \quad R(K)_C = 0.949^{+0.048}_{-0.047} , \quad (2)$$

$$R(K^*)_L = 0.927^{+0.099}_{-0.093} , \quad R(K^*)_C = 1.027^{+0.077}_{-0.073} , \quad (3)$$

where  $L(C)$  means the low (central)  $q^2$  region,  $[0.1, 1.1]$   $\text{GeV}^2$  ( $[1.1, 6.0]$   $\text{GeV}^2$ ), turned out to be consistent with the SM predictions. The SM calculations for the  $R(K^{(*)})$  are very close to unity [6–9]

$$\begin{aligned} R(K)_{\text{SM}}[1.0, 6.0] &= 1.0004^{+0.0008}_{-0.0007} , \\ R(K^*)_{\text{SM}}[0.1, 1.1] &= 0.983 \pm 0.014 , \\ R(K^*)_{\text{SM}}[1.1, 6.0] &= 0.996^{+0.002}_{-0.002} . \end{aligned} \quad (4)$$

Also the CMS collaboration measured  $R(K)_C$  as [10]

$$R(K)_C = 0.78^{+0.47}_{-0.23} , \quad (5)$$

which is compatible with the SM. Closely related process is  $B_s \rightarrow \mu^+\mu^-$  decay. The world average of the experimental branching ratio is [11]

$$\text{Br}(B_s \rightarrow \mu^+\mu^-)_{\text{exp}} = (3.34 \pm 0.27) \times 10^{-9} , \quad (6)$$

which is in agreement with the SM result of [12]

$$\text{Br}(B_s \rightarrow \mu^+\mu^-)_{\text{SM}} = (3.64 \pm 0.12) \times 10^{-9} . \quad (7)$$

On the other hand, Belle II Collaboration recently measured  $B \rightarrow K\nu\nu$  branching ratios as [13]

$$\text{Br}(B^+ \rightarrow K^+\nu\bar{\nu})_{\text{exp}} = (2.3 \pm 0.7) \times 10^{-5} , \quad (8)$$

which exceeds the SM predictions [14]

$$\text{Br}(B^+ \rightarrow K^+\nu\bar{\nu})_{\text{SM}} = (4.43 \pm 0.31) \times 10^{-6} . \quad (9)$$

Thus the NP effects, if exist, are suppressed in  $R(K^{(*)})$  and  $\text{Br}(B_s \rightarrow \mu^+\mu^-)$  while enhanced in  $\text{Br}(B^+ \rightarrow K^+\nu\bar{\nu})$ . It would be quite interesting to deal with both opposite trends simultaneously. There have been many studies of NP effects on  $b \rightarrow s$  transition processes: supersymmetry (SUSY) [15–17], the leptoquark (LQ) [18–28],  $Z'$  model [29–35], new scalar models [36–39], and unparticles [40], etc.

In previous works of [41, 42] we analyzed  $R(K^{(*)})$  in a more generic way where NP effects are encoded in the relevant Wilson coefficients as  $C_j^{\text{NP}} \sim (v/M_{\text{NP}})^\alpha$ . Here  $v$  is the SM vacuum expectation value and  $M_{\text{NP}}$  is the NP scale. Inspired by unparticle scenario,  $\alpha$  can be a non-integer parameter. Ordinary NP particles would contribute with  $\alpha = 2$  at tree level. Since  $R(K^{(*)})$  and  $\text{Br}(B_s \rightarrow \mu^+\mu^-)$  tend to suppress NP effects, they would impose lower bounds on  $M_{\text{NP}}$  assuming reasonably finite fermionic couplings. On the contrary  $\text{Br}(B^+ \rightarrow K^+\nu\bar{\nu})$  favors finite NP effects so that it would also constrain upper bounds of  $M_{\text{NP}}$ . In this way we can estimate allowed windows of  $M_{\text{NP}}$  up to involved fermionic couplings. One could easily check the validity of some NP models with this generic framework.

The paper is organized as follows. In the next Section the decay rates for  $B \rightarrow K^{(*)}\ell^+\ell^-$ ,  $B_s \rightarrow \mu^+\mu^-$ , and  $B^+ \rightarrow K^+\nu\bar{\nu}$  are provided. NP effects are parametrized as mentioned above. Section III discusses our results and their physical meanings. In Sec. IV we conclude.

## II. DECAY RATES

The  $b \rightarrow s\ell^+\ell^-$  transition can be described by the following effective Hamiltonian

$$\mathcal{H}_{\text{eff}}(b \rightarrow s\ell\ell) = -\frac{4G_F}{\sqrt{2}}V_{tb}V_{ts}^* \sum_i [C_i(\mu)\mathcal{O}_i(\mu) + C'_i(\mu)\mathcal{O}'_i(\mu)] . \quad (10)$$

For  $R(K^{(*)})$  the relevant operators are [3, 43, 44]

$$\begin{aligned} \mathcal{O}_9 &= \frac{e^2}{16\pi^2} (\bar{s}\gamma^\mu P_L b) (\bar{\ell}\gamma_\mu \ell) , \\ \mathcal{O}_{10} &= \frac{e^2}{16\pi^2} (\bar{s}\gamma^\mu P_L b) (\bar{\ell}\gamma_\mu \gamma_5 \ell) . \end{aligned} \quad (11)$$

The primed operators are proportional to the right-handed quarks,  $\mathcal{O}'_{9,10} \sim (\bar{s}\gamma^\mu P_R b)$ . In this analysis we do not consider  $\mathcal{O}'_{9,10}$  operators for simplicity. One can expand the matrix elements for  $B \rightarrow K^{(*)}$  as [45]

$$\langle K(p) | \bar{s} \gamma_\mu b | B(p_B) \rangle = f_+ \left[ (p_B + p)_\mu - \frac{m_B^2 - m_K^2}{s} q_\mu \right] + \frac{m_B^2 - m_K^2}{s} f_0 q_\mu, \quad (12)$$

$$\langle K(p) | \bar{s} \sigma_{\mu\nu} q^\nu (1 + \gamma_5) b | B(p_B) \rangle = i \left[ (p_B + p)_\mu s - q_\mu (m_B^2 - m_K^2) \right] \frac{f_T}{m_B + m_K}, \quad (13)$$

$$\begin{aligned} \langle K^*(p) | (V - A)_\mu | B(p_B) \rangle &= -i \epsilon_\mu^* (m_B + m_{K^*}) A_1 + i (p_B + p)_\mu (\epsilon^* \cdot p_B) \frac{A_2}{m_B + m_{K^*}} \\ &+ i q_\mu (\epsilon^* \cdot p_B) \frac{2m_{K^*}}{s} (A_3 - A_0) + \frac{\epsilon_{\mu\nu\rho\sigma} \epsilon^{*\nu} p_B^\rho b^\sigma}{m_B + m_{K^*}} 2V, \end{aligned} \quad (14)$$

where  $f_{+,0,T}(s)$ ,  $A_{0,1,2}(s)$ ,  $T_{1,2,3}(s)$ ,  $V(s)$ , and  $f_- = (f_0 - f_+)(1 - \hat{m}_K^2)/\hat{s}$  are the form factors. Here,

$$q = p_B - p, \quad s = q^2 = (p_B - p)^2, \quad (15)$$

$$\hat{s} = \frac{s}{m_B^2}, \quad \hat{m}_i = \frac{m_i}{m_B}. \quad (16)$$

The form factors are functions of  $s$  and we choose the exponential form as [45]

$$F(\hat{s}) = F(0) \exp\left(c_1 \hat{s} + c_2 \hat{s}^2 + c_3 \hat{s}^3\right), \quad (17)$$

where  $c_i$  are the related coefficients.

The differential decay rates for  $B \rightarrow K^{(*)} \ell^+ \ell^-$  with respect to  $s$  are given by [46]

$$\begin{aligned} \frac{d\Gamma_K}{d\hat{s}} &= \frac{G_F^2 \alpha^2 m_B^5}{2^{10} \pi^5} |V_{tb} V_{ts}^*|^2 \hat{u}_{K,\ell} \left\{ (|A'|^2 + |C'|^2) \left( \lambda_K - \frac{\hat{u}_{K,\ell}^2}{3} \right) + |C'|^2 4\hat{m}_\ell^2 (2 + 2\hat{m}_K^2 - \hat{s}) \right. \\ &\left. + \text{Re}(C' D^*) 8\hat{m}_\ell^2 (1 - \hat{m}_K^2) + |D'|^2 4\hat{m}_\ell^2 \hat{s} \right\}, \end{aligned} \quad (18)$$

$$\begin{aligned} \frac{d\Gamma_{K^*}}{d\hat{s}} &= \frac{G_F^2 \alpha^2 m_B^5}{2^{10} \pi^5} |V_{tb} V_{ts}^*|^2 \hat{u}_{K^*,\ell} \left\{ \frac{|A|^2}{3} \hat{s} \lambda_{K^*} \left( 1 + \frac{2\hat{m}_\ell^2}{\hat{s}} \right) + |E|^2 \hat{s} \frac{\hat{u}_{K^*,\ell}^2}{3} \right. \\ &+ \frac{|B|^2}{4\hat{m}_{K^*}^2} \left[ \lambda_{K^*} - \frac{\hat{u}_{K^*,\ell} t^2}{3} + 8\hat{m}_{K^*}^2 (\hat{s} + 2\hat{m}_\ell^2) \right] + \frac{|F|^2}{4\hat{m}_{K^*}^2} \left[ \lambda_{K^*} - \frac{\hat{u}_{K^*,\ell}^2}{3} + 8\hat{m}_{K^*}^2 (\hat{s} - 4\hat{m}_\ell^2) \right] \\ &+ \frac{\lambda_{K^*} |C|^2}{4\hat{m}_{K^*}^2} \left( \lambda_{K^*} - \frac{\hat{u}_{K^*,\ell}^2}{3} \right) + \frac{\lambda_{|K^*|G|^2}}{4\hat{m}_{K^*}^2} \left[ \lambda_{K^*} - \frac{\hat{u}_{K^*,\ell}^2}{3} + 4\hat{m}_\ell^2 (2 + 2\hat{m}_{K^*}^2 - \hat{s}) \right] \\ &- \frac{\text{Re}(BC^*)}{2\hat{m}_{K^*}^2} \left( \lambda_{K^*} - \frac{\hat{u}_{K^*,\ell}^2}{3} \right) (1 - \hat{m}_{K^*}^2 - \hat{s}) \\ &- \frac{\text{Re}(FG^*)}{2\hat{m}_{K^*}^2} \left[ \left( \lambda_{K^*} - \frac{\hat{u}_{K^*,\ell}^2}{3} \right) (1 - \hat{m}_{K^*}^2 - \hat{s}) - 4\hat{m}_\ell^2 \lambda_{K^*} \right] \\ &\left. - \frac{2\hat{m}_\ell^2}{\hat{m}_{K^*}^2} \lambda_{K^*} \left[ \text{Re}(FH^*) - \text{Re}(GH^*) (1 - \hat{m}_{K^*}^2) \right] + \frac{\hat{m}_\ell^2}{\hat{m}_{K^*}^2} \hat{s} \lambda_{K^*} |H|^2 \right\}, \end{aligned} \quad (19)$$

where the kinematic variables are

$$\lambda_H = 1 + \hat{m}_H^4 + \hat{s}^2 - 2\hat{s} - 2\hat{m}_H^2(1 + \hat{s}) , \quad (20)$$

$$\hat{u}_{H,\ell} = \sqrt{\lambda_H \left(1 - \frac{4\hat{m}_\ell^2}{\hat{s}}\right)} . \quad (21)$$

Here  $A', \dots, D'$  and  $A, \dots, H$  are the auxiliary functions. They are defined by the form factors combined with the Wilson coefficients as [45],

$$A' = C_9 f_+ + \frac{2\hat{m}_b}{1 + \hat{m}_K} C_7^{\text{eff}} f_T , \quad (22)$$

$$B' = C_9 f_- - \frac{2\hat{m}_b}{\hat{s}} (1 - \hat{m}_K) C_7^{\text{eff}} f_T , \quad (23)$$

$$C' = C_{10} f_+ , \quad (24)$$

$$D' = C_{10} f_- , \quad (25)$$

and

$$A = \frac{2}{1 + \hat{m}_{K^*}} C_9 V + \frac{4\hat{m}_b}{\hat{s}} C_7^{\text{eff}} T_1 , \quad (26)$$

$$B = (1 + \hat{m}_{K^*}) \left[ C_9 A_1 + \frac{2\hat{m}_b}{\hat{s}} (1 - \hat{m}_{K^*}) C_7^{\text{eff}} T_2 \right] , \quad (27)$$

$$C = \frac{1}{1 - \hat{m}_{K^*}^2} \left[ (1 - \hat{m}_{K^*}) C_9 A_2 + 2\hat{m}_b C_7^{\text{eff}} \left( T_3 + \frac{1 - \hat{m}_{K^*}^2}{\hat{s}} T_2 \right) \right] , \quad (28)$$

$$D = \frac{1}{\hat{s}} \{ C_9 [(1 + \hat{m}_{K^*}) A_1 - (1 - \hat{m}_{K^*}) A_2 - 2\hat{m}_{K^*} A_0] - 2\hat{m}_b C_7^{\text{eff}} T_3 \} , \quad (29)$$

$$E = \frac{2}{1 + \hat{m}_{K^*}} C_{10} V , \quad (30)$$

$$F = (1 + \hat{m}_{K^*}) C_{10} A_1 , \quad (31)$$

$$G = \frac{1}{1 + \hat{m}_{K^*}} C_{10} A_2 , \quad (32)$$

$$H = \frac{1}{\hat{s}} C_{10} [(1 + \hat{m}_{K^*}) A_1 - (1 - \hat{m}_{K^*}) A_2 - 2\hat{m}_{K^*} A_0] . \quad (33)$$

Possible NP effects on  $R(K^{(*)})$  could also affect the  $B_s \rightarrow \mu^+ \mu^-$  decay. In this case NP enters via a new Wilson coefficient  $C_{10}^{\text{NP}}$  in the branching ratio

$$\text{Br}(B_s \rightarrow \mu^+ \mu^-) = \text{Br}(B_s \rightarrow \mu^+ \mu^-)_{\text{SM}} \left| 1 + \frac{C_{10}^{\mu\text{NP}}}{C_{10}^{\mu\text{SM}}} \right|^2 , \quad (34)$$

where  $C_{10}^{\mu\text{SM}}$  is the SM value of  $C_{10}^\mu$ ,  $C_{10}^{\mu\text{SM}} = -4.41$  [47, 48].

Now we parameterize the Wilson coefficient as mentioned in Sec. I,

$$C_{9,10}^{\ell,\text{NP}} = \mathcal{N} A_{9,10}^\ell \left( \frac{v}{M_{\text{NP}}} \right)^\alpha , \quad (35)$$

where  $\ell = e, \mu$  and  $\mathcal{N} = |\alpha_{em} V_{tb} V_{ts}^*|^{-1}$ . Here  $M_{\text{NP}}$  is the NP scale and  $A_{9,10}^\ell$  are the involved coefficients, and  $\alpha$  is a free parameter.  $A_{9,10}^\ell$  involve the fermionic couplings to NP. In general NP effects could exist in the electron sector with  $A_{9,10}^e \neq 0$ . But non-zero  $A_{9,10}^e$  would affect the electron dipole moment which is in very good agreement with the SM. So we simply assume that the NP appears only in the muon sector putting  $A_{9,10}^e = 0$ , and we drop the superscript  $\ell$  or  $\mu$  in what follows.

In principle it is possible that NP could appear in  $C_7$ . But as discussed in [16, 42], the constraint on  $C_7$  from  $B \rightarrow X_s \gamma$  is so strong that there is very little room for NP in  $C_7$ , so we neglect possible NP in  $C_7$ .

Now let's move to  $b \rightarrow s \nu \nu$  decay. The relevant effective Hamiltonian is [49, 50]

$$\mathcal{H}_{\text{eff}}(b \rightarrow s \nu \nu) = \frac{4G_F}{\sqrt{2}} \frac{e^2}{(4\pi)^2} V_{tb} V_{ts}^* \sum_{k=L,R} \sum_{i,j} C_{\nu k}^{ij} [\bar{s} \gamma_\mu P_k b] [\bar{\nu}_i \gamma^\mu (1 - \gamma_5) \nu_j] + \text{h.c.} . \quad (36)$$

The branching ratio of  $B \rightarrow K \nu \nu$  is [14, 49]

$$\text{Br}(B \rightarrow K \nu \nu) = \text{Br}(B \rightarrow K \nu \nu)_{\text{SM}} \frac{1}{3 |C_{\nu L}^{\text{SM}}|^2} \sum_{i,j} \left| C_{\nu L}^{ij} + C_{\nu R}^{ij} \right|^2, \quad (37)$$

where  $C_{\nu L}^{ij} = C_{\nu L}^{\text{SM}} \delta^{ij} + \delta C_{\nu L}^{ij}$  and  $C_{\nu L}^{\text{SM}}$  is the SM Wilson coefficient,  $C_{\nu L}^{\text{SM}} = -6.32$  [50]. The NP effects appear through  $\delta C_{\nu L}^{ij}$  and  $C_{\nu R}^{ij}$ . We can expand the branching ratio as follows:

$$\text{Br}(B \rightarrow K \nu \nu) = \text{Br}(B \rightarrow K \nu \nu)_{\text{SM}} \left| 1 + L + Q \right|, \quad (38)$$

where linear(L) and quadratic(Q) terms of  $C_{\nu}$ s are parameterized as

$$\begin{aligned} L &= \frac{\mathcal{N}}{C_L^{\text{SM}}} A_L \left( \frac{v}{M_{\text{NP}}} \right)^\alpha, \\ Q &= \left| \frac{\mathcal{N}}{C_L^{\text{SM}}} \right|^2 A_Q \left( \frac{v}{M_{\text{NP}}} \right)^{2\alpha}. \end{aligned} \quad (39)$$

### III. RESULTS AND DISCUSSIONS

We implement the  $\chi^2$  fit for  $R(K^{(*)})$  and the branching ratios  $\text{Br}(B_s \rightarrow \mu^+ \mu^-)$  and  $\text{Br}(B^+ \rightarrow K^+ \nu \bar{\nu})$ . The scan range covers  $0 \leq \alpha \leq 5$ ,  $1 \text{ TeV} \leq M_{\text{NP}} \leq 50 \text{ TeV}$ ,  $|A_{9,10}| \leq 1$ ,  $|A_L| \leq 10$ , and  $|A_Q| \leq 10^2$ . The best-fit values are summarized in Table I. The minimum value of  $\chi^2$  per d.o.f is  $\chi_{\text{min}}^2/\text{d.o.f} = 1.37$ . The best-fit  $\alpha_{\text{best}}$  is less than 2. The best-fit  $M_{\text{NP,best}}$  is 26.4 TeV. If  $\alpha_{\text{best}}$  were larger then  $M_{\text{NP,best}}$  would be smaller.

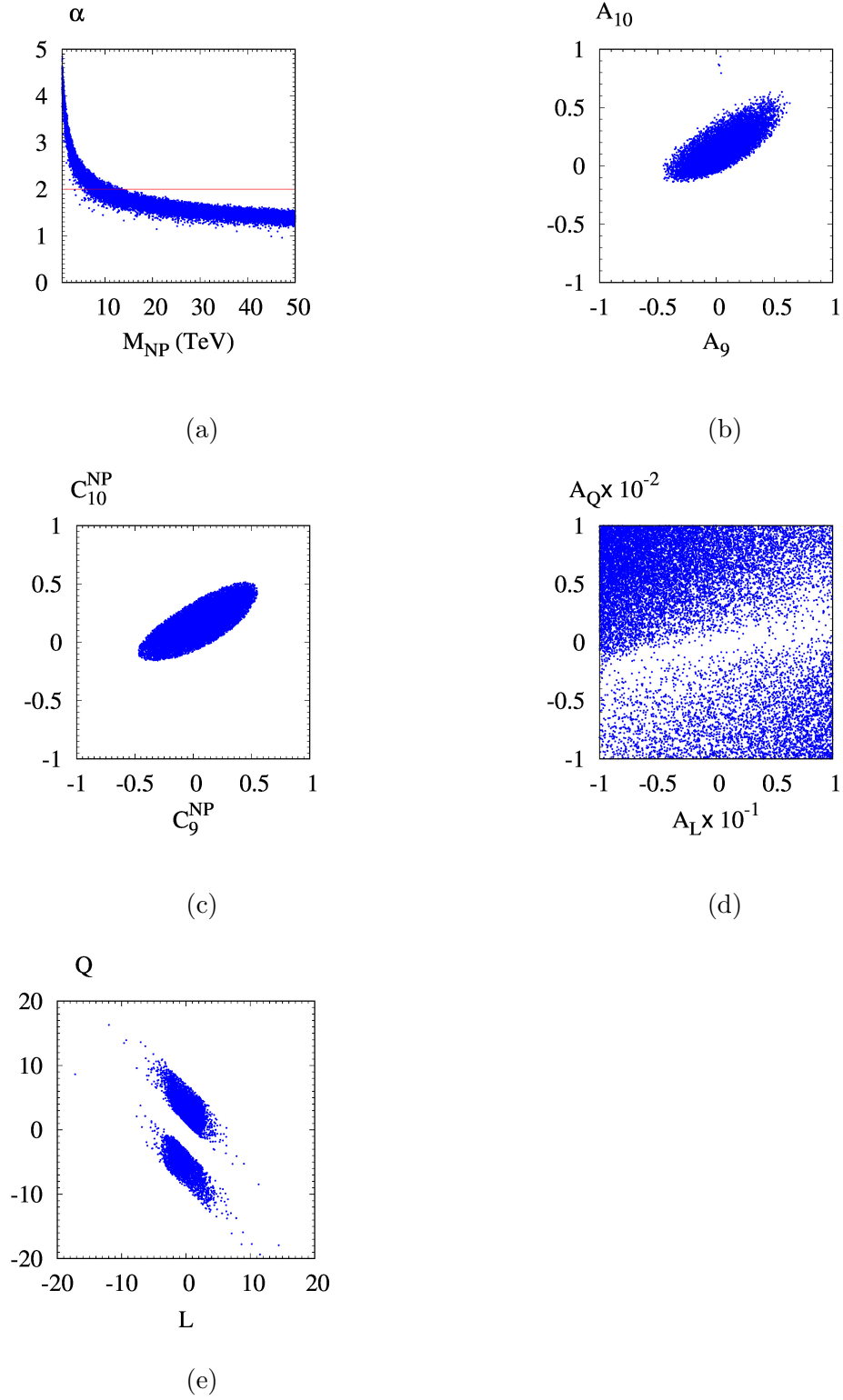


FIG. 1. Allowed regions of (a)  $\alpha$  vs.  $M_{\text{NP}}$ , (b)  $A_{10}$  vs.  $A_9$ , (c)  $C_{10}^{\text{NP}}$  vs.  $C_9^{\text{NP}}$ , (d)  $A_Q$  vs.  $A_L$ , and (e)  $Q$  vs.  $L$  at the  $2\sigma$  level.

$\alpha$	1.53	$R(K)_L$	0.971
$M_{\text{NP}}$ (TeV)	26.4	$R(K)_C$	0.978
$A_9$	0.064	$R(K^*)_L$	0.918
$A_{10}$	0.115	$R(K^*)_C$	0.967
$A_L \times 10$	0.791	$\text{Br}(B_s \rightarrow \mu\mu)$	$3.36 \times 10^{-9}$
$A_Q \times 10^2$	-0.722	$\text{Br}(B \rightarrow K\nu\nu)$	$2.29 \times 10^{-5}$
$C_9$	0.099	$C_{10}$	0.176

TABLE I. Best-fit values of our fitting.

Figure 1 shows the allowed regions of the fitting parameters, Wilson coefficients,  $L$ , and  $Q$  at the  $2\sigma$  level. In Fig. 1 (a),  $\alpha$  and  $M_{\text{NP}}$  show a typical exponential behavior. One point to note is that for those vales of  $\alpha \gtrsim 1.6$  the allowed  $M_{\text{NP}}$  has an upper bound. This is mainly because  $\text{Br}(B \rightarrow K\nu\nu)_{\text{exp}}$  is far away from the SM calculations. If NP could explain the discrepancy, its effect should be large enough. To make it happen for moderate values of the relevant couplings,  $M_{\text{NP}}$  must be bounded from above. If we do not consider  $B^+ \rightarrow K^+\nu\bar{\nu}$  process, then one can find no upper bounds of  $M_{\text{NP}}$ .

As shown in Fig. 1 (b),  $A_{10}$  favors positive values. It reflects the fact that the experimental data of  $\text{Br}(B_s \rightarrow \mu\mu)$  are slightly smaller than the SM predictions. Note that  $C_{10}^{\text{SM}}$  in  $\text{Br}(B_s \rightarrow \mu^+\mu^-)$  is negative. In Fig. 1 (c) there are very few points around  $C_{10}^{\text{NP}} \sim 8.5$  which are not shown here. Those few points are possible because the branching ratio  $\text{Br}(B_s \rightarrow \mu\mu)$  is proportional to  $\sim \left|1 + C_{10}^{\text{NP}}/C_{10}^{\text{SM}}\right|^2$ , and we have two solutions of positive and negative  $\left(1 + C_{10}^{\text{NP}}/C_{10}^{\text{SM}}\right)$ . Large  $C_{10}^{\text{NP}}$  corresponds to the negative solution (note that  $C_{10}^{\text{SM}} < 0$ ). See Figs. 2 (c) and (d) of [42]. In Figs. 1 (d) and (e) there are narrow strips of rare points which are not allowed by our fitting. They correspond to the line of  $L + Q = 0$  in Eq. (38) for which NP effects vanish.

In Fig. 2, we plot the allowed regions of the observables. As shown in Fig. 2 (a) and (c), in our fitting  $R(K^*)_L$  and  $\text{Br}(B \rightarrow K\nu\nu)$  have no overlaps with the SM predictions while  $R(K)_L$ ,  $R(K^*)_C$  and  $\text{Br}(B_s \rightarrow \mu^+\mu^-)$  are quite compatible with SM. While the experimental data of  $R(K^*)_L$  in Eq. (2) are compatible with the SM, the central value of it is rather smaller than the SM compared to other data.

Figure 3 provides  $A_j$  vs.  $M_{\text{NP}}$  for fixed  $\alpha = 2$ . This is the case for ordinary new particle



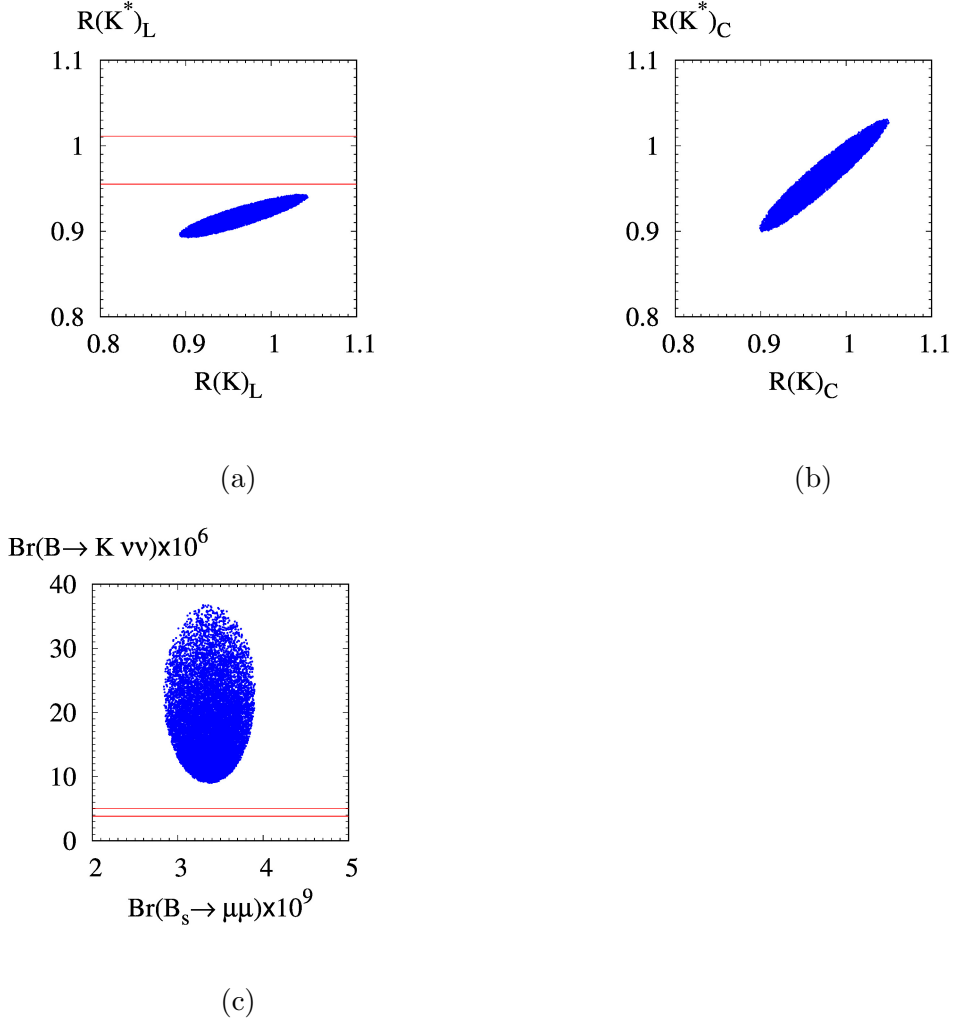


FIG. 2. Allowed regions of (a)  $R(K^*)_L$  vs.  $R(K)_L$ , (b)  $R(K^*)_C$  vs.  $R(K)_C$ , and (c)  $\text{Br}(B \rightarrow K\nu\nu) \times 10^6$  vs.  $\text{Br}(B_s \rightarrow \mu\mu) \times 10^9$  at the  $2\sigma$  level. Horizontal lines show the SM ranges in  $2\sigma$  of  $R(K^*)_L$  in (a) and of  $\text{Br}(B \rightarrow K\nu\nu)$  in (c).

contributions. Note that in case of  $\alpha = 2$ ,  $M_{\text{NP}}$  is restricted from above and below. This is expected in Fig. 1 (a). For  $\alpha = 2$ , we have

$$3.17 \text{ TeV} \leq M_{\text{NP}} \leq 14.9 \text{ TeV} . \quad (40)$$

Comparing Figs. 3 (a) and (b) with (c) and (d),  $M_{\text{NP}}$  is more sensitive to  $A_{L,Q}$  in the sense that for larger  $|A_{L,Q}|$ , the upper bound of  $M_{\text{NP}}$  also gets larger. The feature can also be seen in Figs. 3 (e) and (f). As for  $A_{9,10}$ , they are responsible for  $R(K^{(*)})$  and  $\text{Br}(B_s \rightarrow \mu^+\mu^-)$  which are in agreement with the SM. Thus  $A_{9,10}$  are much more involved in the lower bound of  $M_{\text{NP}}$  for which  $A_{9,10}$  get close to zero as shown in Figs. 3 (a) and (b). On the contrary,

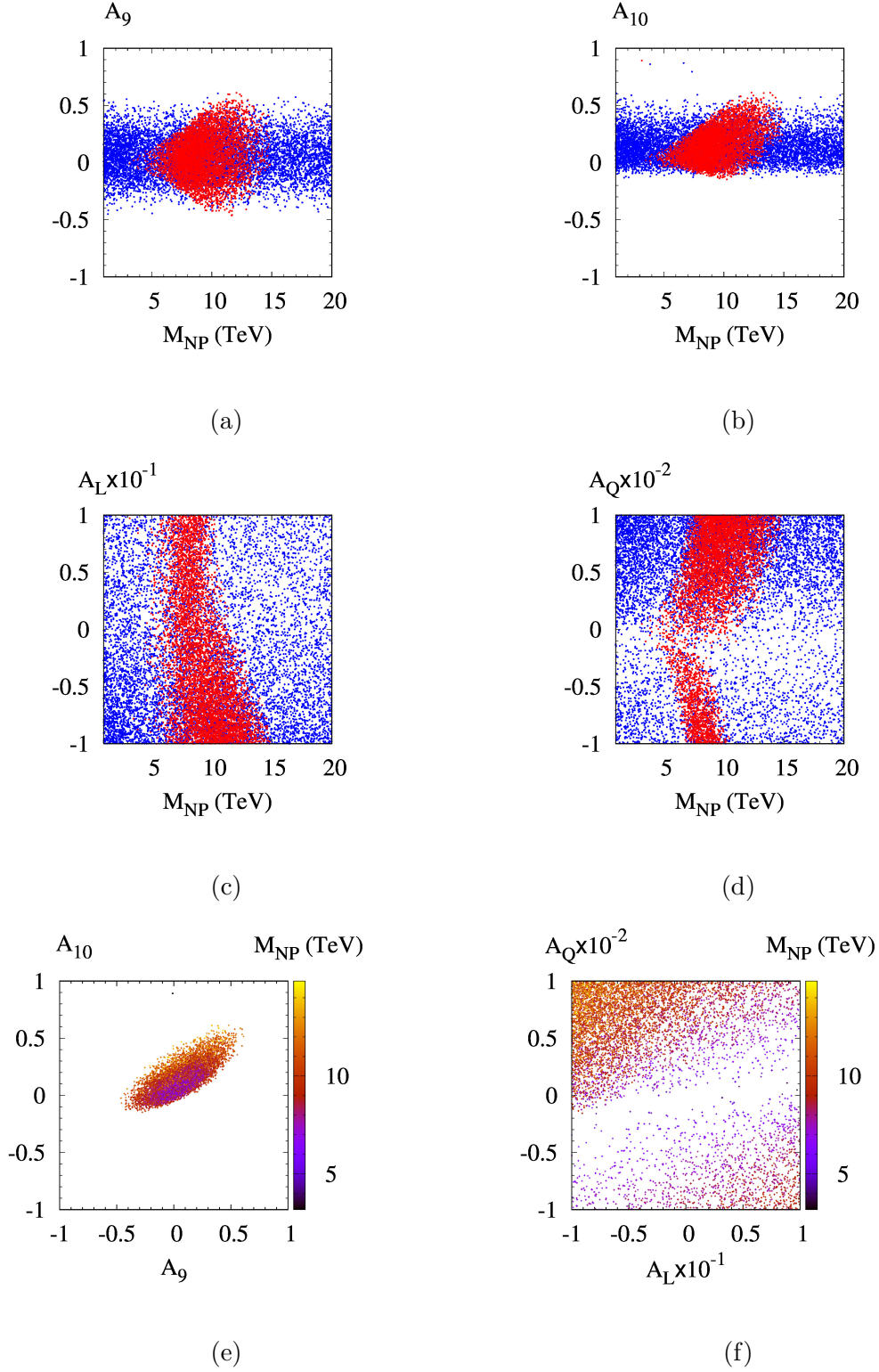


FIG. 3. Allowed regions (at the  $2\sigma$  level) of (a)  $A_9$  vs.  $M_{\text{NP}}$ , (b)  $A_{10}$  vs.  $M_{\text{NP}}$ , (c)  $A_L$  vs.  $M_{\text{NP}}$ , and (d)  $A_Q$  vs.  $M_{\text{NP}}$  for free  $\alpha$  (blue) and fixed  $\alpha = 2$  (red) respectively; (e)  $A_{10}$  vs.  $A_9$  with respect to  $M_{\text{NP}}$ , and (f)  $A_Q$  vs.  $A_L$  with respect to  $M_{\text{NP}}$  for fixed  $\alpha = 2$ .

$A_{L,Q}$  are responsible for  $\text{Br}(B^+ \rightarrow K^+\nu\bar{\nu})$  that deviates from the SM, which makes  $A_{L,Q}$  much more involved with the upper bound of  $M_{\text{NP}}$ . As for  $\text{Br}(B \rightarrow K\nu\nu)$  finite NP effects should be maintained to accommodate the experimental data, so for given  $A_{L,Q}$ ,  $M_{\text{NP}}$  could not be large enough. This is the origin of the upper bound of  $M_{\text{NP}}$ . According to Figs. 3 (c), (d) and (f), negative  $A_L$  and positive  $A_Q$  are more involved with the upper bound of  $M_{\text{NP}}$ . These parts tend to enhance  $\text{Br}(B^+ \rightarrow K^+\nu\bar{\nu})$  in Eq. (38) to come up with the experimental data.

It is quite remarkable that our generic analysis puts a window of allowed  $M_{\text{NP}}$  with the width of  $\sim 12$  TeV. Using the window one can check the validity of various NP scenarios with their couplings and NP scales which are constrained by other experimental data.

Figure 4 plots the allowed regions of observables with respect to  $M_{\text{NP}}$  for fixed  $\alpha = 2$ . For larger values of  $M_{\text{NP}}$ , allowed regions of  $R(K^{(*)})$  and the branching ratios of  $B_s \rightarrow \mu^+\mu^-$  and  $B^+ \rightarrow K^+\nu\bar{\nu}$  get smaller. This is because the NP effects tend to diminish for larger  $M_{\text{NP}}$ . Compared with Fig. 2, fixing  $\alpha = 2$  has almost no effects on the allowed regions of  $R(K^{(*)})_{L,C}$  and the branching ratios  $\text{Br}(B_s \rightarrow \mu\nu)$  and  $\text{Br}(B \rightarrow K\nu\nu)$ . It means that although  $\alpha$  is fixed to 2, other parameters can cover the observables but the allowed regions of them are shrunk much, as shown in Fig. 3.

Our approach can be used as a toolkit to test the validity of specific NP models. For example, allowed  $Z'$  mass for explaining  $(g-2)_\mu$  from  $U(1)_{B_2-L_\mu}$  model in [34] is  $m_{Z'} < 300$  GeV for a coupling of unity. This is off from our suggested range of  $M_{\text{NP}}$ . On the other hand, a vector LQ of [27] compatible with  $(g-2)_\mu$  and various  $B$  anomalies including  $R(K^{(*)})$  is estimated to have its mass from 1.5 TeV to several TeV. The range is quite challenging in view of our window if the lower bound is  $\sim 3.2$  TeV. In a similar manner one can check directly the compatibility of other NP models with  $R(K^{(*)})$ ,  $\text{Br}(B_s \rightarrow \mu^+\mu^-)$ , and  $\text{Br}(B^+ \rightarrow K^+\nu\bar{\nu})$ .

#### IV. CONCLUSIONS

In conclusion, we investigated possible NP effects on  $b \rightarrow s$  transition processes. Experimental data of the ratio  $R(K^{(*)})$  and  $\text{Br}(B_s \rightarrow \mu^+\mu^-)$  are compatible with the SM predictions while  $\text{Br}(B^+ \rightarrow K^+\nu\bar{\nu})$  needs NP to explain the discrepancy of experiment and theory. Considering these two kinds of data simultaneously turned out to be very interesting

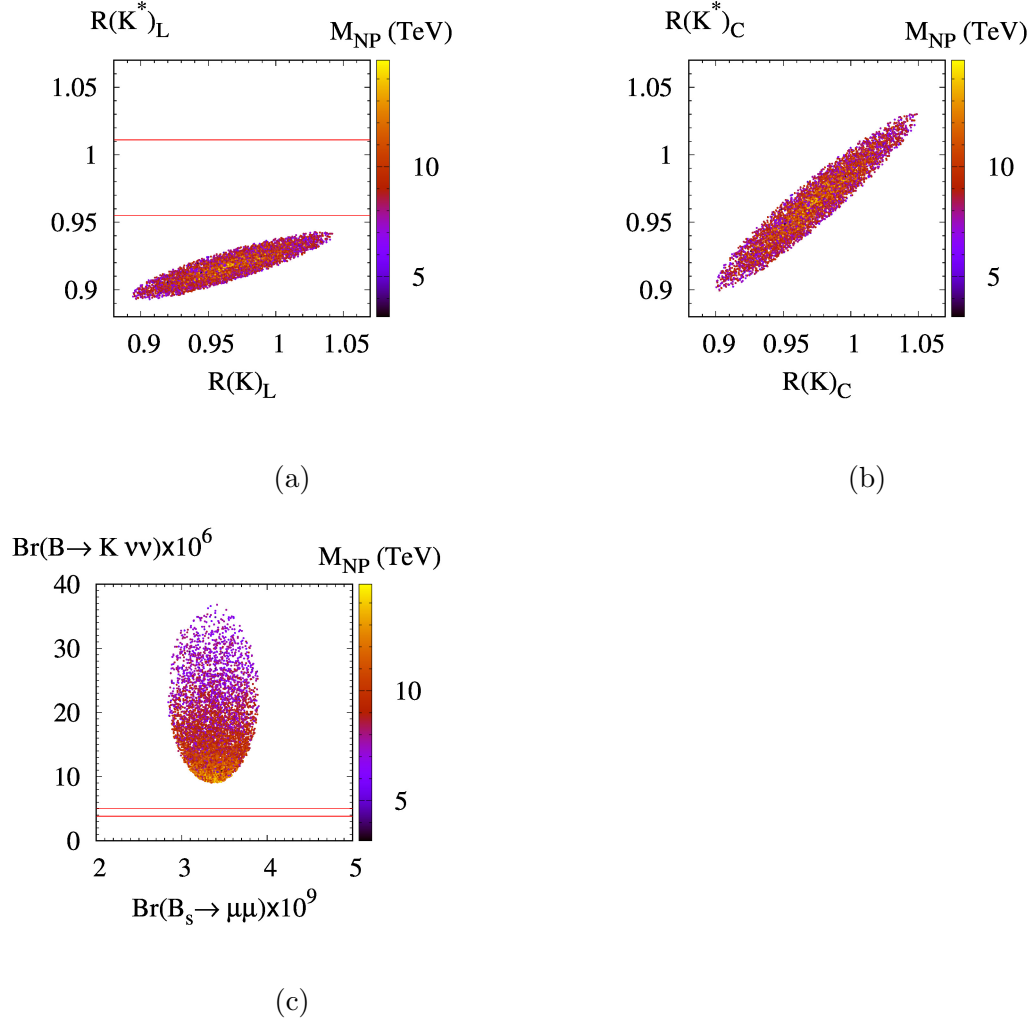


FIG. 4. Allowed regions of (a)  $R(K^*)_L$  vs.  $R(K)_L$  with respect to  $M_{\text{NP}}$ , (b)  $R(K^*)_C$  vs.  $R(K)_C$  with respect to  $M_{\text{NP}}$ , and (c)  $\text{Br}(B \rightarrow K \nu \nu)$  vs.  $\text{Br}(B_s \rightarrow \mu \mu)$  with respect to  $M_{\text{NP}}$  at the  $2\sigma$  level for fixed  $\alpha = 2$ . Horizontal lines show the SM ranges in  $2\sigma$  of  $R(K^*)_L$  in (a) and of  $\text{Br}(B \rightarrow K \nu \nu)$  in (c).

with regard to NP scale. We parameterized NP effects in a generic way with NP scale  $M_{\text{NP}}$  explicitly with some possible power  $\alpha$  of it. Our best-fit value of  $\alpha$  is less than 2 which corresponds to the case of ordinary new particles. For a reasonable range of NP fermionic couplings we found that  $3.17 \text{ TeV} \leq M_{\text{NP}} \leq 14.9 \text{ TeV}$  for ordinary NP particles contributing at tree level. The window of  $M_{\text{NP}}$  would vary for different ranges of couplings. Since the width of the allowed window of  $M_{\text{NP}}$  is not so wide, our results would be very helpful to check validity of various NP scenarios in a generic way. If new particles contribute via loop processes, then the NP scale would appear in a more complicated form, which is beyond our

current analysis.

For specific NP models one should include constraints from  $B^0 \rightarrow K^{*0}\nu\bar{\nu}$  decays. Experimentally we have an upper bound of  $\text{Br}(B^0 \rightarrow K^{*0}\nu\bar{\nu}) < 1.8 \times 10^{-5}$  [51]. Future measurements will cast much more information for NP contributions.

## ACKNOWLEDGMENTS

This paper was supported by Konkuk University in 2024.

- 
- [1] R. Aaij *et al.* [LHCb], JHEP **08** (2017), 055.
  - [2] R. Aaij *et al.* [LHCb], Nature Phys. **18**, no.3, 277-282 (2022).
  - [3] L. S. Geng, B. Grinstein, S. Jäger, S. Y. Li, J. Martin Camalich and R. X. Shi, Phys. Rev. D **104**, no.3, 035029 (2021).
  - [4] R. Aaij *et al.* [LHCb], Phys. Rev. Lett. **131**, no.5, 051803 (2023).
  - [5] R. Aaij *et al.* [LHCb], Phys. Rev. D **108**, no.3, 032002 (2023).
  - [6] G. Hiller and F. Kruger, Phys. Rev. D **69** (2004), 074020.
  - [7] C. Bobeth, G. Hiller and G. Piranishvili, JHEP **12** (2007), 040.
  - [8] L. S. Geng, B. Grinstein, S. Jäger, J. Martin Camalich, X. L. Ren and R. X. Shi, Phys. Rev. D **96** (2017) no.9, 093006.
  - [9] M. Bordone, G. Isidori and A. Pattori, Eur. Phys. J. C **76**, no.8, 440 (2016).
  - [10] CMS Collaboration, Test of lepton flavor universality in  $B^+ \rightarrow K^+\ell^+\ell^-$  decays, CMS-PAS=BPH-22-005 (2023).
  - [11] S. Navas *et al.* [Particle Data Group], Phys. Rev. D **110**, no.3, 030001 (2024).
  - [12] M. Czaja and M. Misiak, Symmetry **16**, no.7, 917 (2024).
  - [13] I. Adachi *et al.* [Belle-II], Phys. Rev. D **109**, no.11, 112006 (2024).
  - [14] D. Bečirević, G. Piazza and O. Sumensari, Eur. Phys. J. C **83**, no.3, 252 (2023).
  - [15] W. Altmannshofer, P. S. B. Dev, A. Soni and Y. Sui, Phys. Rev. D **102** (2020) no.1, 015031.
  - [16] D. Bardhan, D. Ghosh and D. Sachdeva, Nucl. Phys. B **986**, 116059 (2023).
  - [17] M. D. Zheng, Q. L. Wang, L. F. Lai and H. H. Zhang, [arXiv:2410.04348 [hep-ph]].
  - [18] G. Hiller and M. Schmaltz, Phys. Rev. D **90** (2014), 054014.

- [19] I. Doršner, S. Fajfer, A. Greljo, J. F. Kamenik and N. Košnik, Phys. Rept. **641** (2016), 1-68.
- [20] M. Bauer and M. Neubert, Phys. Rev. Lett. **116** (2016) no.14, 141802.
- [21] C. H. Chen, T. Nomura and H. Okada, Phys. Lett. B **774** (2017), 456-464.
- [22] A. Crivellin, D. Müller and T. Ota, JHEP **09** (2017), 040.
- [23] L. Calibbi, A. Crivellin and T. Li, Phys. Rev. D **98** (2018) no.11, 115002.
- [24] M. Blanke and A. Crivellin, Phys. Rev. Lett. **121** (2018) no.1, 011801.
- [25] T. Nomura and H. Okada, Phys. Rev. D **104**, no.3, 035042 (2021).
- [26] A. Angelescu, D. Bečirević, D. A. Faroughy, F. Jaffredo and O. Sumensari, Phys. Rev. D **104**, no.5, 055017 (2021).
- [27] M. Du, J. Liang, Z. Liu and V. Tran, [arXiv:2104.05685 [hep-ph]].
- [28] K. Cheung, W. Y. Keung and P. Y. Tseng, Phys. Rev. D **106**, no.1, 015029 (2022).
- [29] A. Crivellin, G. D'Ambrosio and J. Heeck, Phys. Rev. Lett. **114** (2015), 151801.
- [30] A. Crivellin, G. D'Ambrosio and J. Heeck, Phys. Rev. D **91** (2015) no.7, 075006.
- [31] C. W. Chiang, X. G. He, J. Tandean and X. B. Yuan, Phys. Rev. D **96** (2017) no.11, 115022.
- [32] S. F. King, JHEP **08** (2017), 019.
- [33] R. S. Chivukula, J. Isaacson, K. A. Mohan, D. Sengupta and E. H. Simmons, Phys. Rev. D **96** (2017) no.7, 075012.
- [34] J. Y. Cen, Y. Cheng, X. G. He and J. Sun, Nucl. Phys. B **978**, 115762 (2022).
- [35] J. Davighi, JHEP **08**, 101 (2021).
- [36] Q. Y. Hu, X. Q. Li and Y. D. Yang, Eur. Phys. J. C **77** (2017) no.3, 190.
- [37] A. Crivellin, D. Müller and C. Wiegand, JHEP **06** (2019), 119.
- [38] L. Delle Rose, S. Khalil, S. J. D. King and S. Moretti, Phys. Rev. D **101** (2020) no.11, 115009.
- [39] S. Y. Ho, J. Kim and P. Ko, [arXiv:2401.10112 [hep-ph]].
- [40] J. P. Lee, Mod. Phys. Lett. A **37**, no.32, 2250214 (2022).
- [41] J. P. Lee, J. Korean Phys. Soc. **80**, no.1, 13-19 (2022).
- [42] J. P. Lee, Mod. Phys. Lett. A **38**, no.16n17, 2350080 (2023).
- [43] R. Alonso, B. Grinstein and J. Martin Camalich, Phys. Rev. Lett. **113** (2014), 241802.
- [44] L. S. Geng, B. Grinstein, S. Jäger, J. Martin Camalich, X. L. Ren and R. X. Shi, Phys. Rev. D **96** (2017) no.9, 093006.
- [45] A. Ali, P. Ball, L. T. Handoko and G. Hiller, Phys. Rev. D **61** (2000), 074024.
- [46] Q. Chang, X. Q. Li and Y. D. Yang, JHEP **04**, 052 (2010).

- [47] D. Becirevic, N. Kosnik, F. Mescia and E. Schneider, *Phys. Rev. D* **86**, 034034 (2012).
- [48] A. D'Alise, G. Fabiano, D. Frattulillo, D. Iacobacci, F. Sannino, P. Santorelli and N. Vignaroli, *Nucl. Phys. B* **1006**, 116631 (2024).
- [49] L. Allwicher, D. Becirevic, G. Piazza, S. Rosauero-Alcaraz and O. Sumensari, *Phys. Lett. B* **848**, 138411 (2024)
- [50] O. Sumensari, [arXiv:2406.00218 [hep-ph]].
- [51] J. Grygier *et al.* [Belle], *Phys. Rev. D* **96**, no.9, 091101 (2017).